New Mexico Geological Society

Downloaded from: https://nmgs.nmt.edu/publications/guidebooks/37



A stratigraphic framework for the eastern Mogollon-Datil volcanic field based on paleomagnetism and high-precision $^{40}Ar/^{39}Ar$ dating of ignimbrites--A progress report

William C. McIntosh, John F. Sutter, Charles E. Chapin, Glenn R. Osburn, and James C. Ratte
1986, pp. 183-195. https://doi.org/10.56577/FFC-37.183

in:

Truth or Consequences Region, Clemons, R. E.; King, W. E.; Mack, G. H.; Zidek, J.; [eds.], New Mexico Geological Society 37th Annual Fall Field Conference Guidebook, 317 p. https://doi.org/10.56577/FFC-37

This is one of many related papers that were included in the 1986 NMGS Fall Field Conference Guidebook.

Annual NMGS Fall Field Conference Guidebooks

Every fall since 1950, the New Mexico Geological Society (NMGS) has held an annual Fall Field Conference that explores some region of New Mexico (or surrounding states). Always well attended, these conferences provide a guidebook to participants. Besides detailed road logs, the guidebooks contain many well written, edited, and peer-reviewed geoscience papers. These books have set the national standard for geologic guidebooks and are an essential geologic reference for anyone working in or around New Mexico.

Free Downloads

NMGS has decided to make peer-reviewed papers from our Fall Field Conference guidebooks available for free download. This is in keeping with our mission of promoting interest, research, and cooperation regarding geology in New Mexico. However, guidebook sales represent a significant proportion of our operating budget. Therefore, only *research papers* are available for download. *Road logs*, *mini-papers*, and other selected content are available only in print for recent guidebooks.

Copyright Information

Publications of the New Mexico Geological Society, printed and electronic, are protected by the copyright laws of the United States. No material from the NMGS website, or printed and electronic publications, may be reprinted or redistributed without NMGS permission. Contact us for permission to reprint portions of any of our publications.

One printed copy of any materials from the NMGS website or our print and electronic publications may be made for individual use without our permission. Teachers and students may make unlimited copies for educational use. Any other use of these materials requires explicit permission.

This page is intentionally left blank to maintain order of facing pages.

A STRATIGRAPHIC FRAMEWORK FOR THE EASTERN MOGOLLON–DATIL VOLCANIC FIELD BASED ON PALEOMAGNETISM AND HIGH-PRECISION $^{40}Ar/^{39}Ar$ DATING OF IGNIMBRITES—A PROGRESS REPORT

WILLIAM C. McINTOSH[1], JOHN F. SUTTER[2], CHARLES E. CHAPIN[1], GLENN R. OSBURN[1] and JAMES C. RATTÉ[3]
[1]New Mexico Bureau of Mines & Mineral Resources, Socorro, NM 87801; [2]U.S. Geological Survey, 981 National Center, Reston, VA 22092;
[3]U.S. Geological Survey, Federal Center, Denver, CO 80225

Abstract—A reliable stratigraphic framework for the Oligocene Mogollon–Datil volcanic field is being developed by correlating ignimbrites (ash-flow tuffs) using existing detailed mapping in conjunction with paleomagnetic measurements and high-precision $^{40}Ar/^{39}Ar$ dating of sanidine separates, which has a relative error of ± 0.15 my or better.

Thirty-three ignimbrite units have been studied, of which at least 27 are stratigraphically distinct. Thus far, the stratigraphy and age of 14 of the units have been tightly constrained. The ages of these units fall into three eruptive intervals.

The early group of ignimbrites was erupted between 35.51 and 33.93 my. Well-dated ignimbrite units emplaced during this interval include Datil Well Tuff (35.51 my), Kneeling Nun Tuff (35.28 my), Tadpole Ridge Tuff (35.14 my), and Blue Canyon Tuff (33.93 my). Polarity of the Datil Well Tuff is normal, and the other three units are reversed. The normal-to-reversed polarity transition at about 35.4 my can be traced throughout many of the older exposed Oligocene sections in the Mogollon–Datil volcanic field.

The middle eruptive interval (<33.93 to >29.03 my) is represented by only one well-dated unit, the Hells Mesa Tuff (32.04 my). The 1.89 and 3.01 my long ignimbrite hiatuses respectively preceding and following the eruption of the Hells Mesa Tuff are well established for the Socorro area and may extend throughout the entire Mogollon–Datil volcanic field.

The late eruptive interval includes at least nine voluminous ignimbrites erupted in the 1.67 my interval between 29.03 and 27.36 my. These units, totaling at least 6,000 km^3, were erupted from calderas in both the Mogollon Mountains and Socorro areas. Well-dated ignimbrites emplaced during this interval include Davis Canyon Tuff (29.03 my), La Jencia Tuff (28.78 my), Vicks Peak Tuff (28.46 my), Shelley Peak Tuff (28.52 my), Bloodgood Canyon Tuff (28.36 my), tuff of Caronita Canyon (27.85 my), Lemitar Tuff (27.97 my), tuff of Triangle C Ranch (27.98 my), and South Canyon Tuff (27.36 my). Only three of these units (tuff of Caronita Canyon, Lemitar Tuff, and tuff of Triangle C Ranch) are normally magnetized. This normal-polarity interval may correlate with sea-floor normal anomaly 10, although the data is not yet sufficient to substantiate this correlation.

Taylor Creek Rhyolites have not been dated in this study, but some of the domes are tightly bracketed by stratigraphic correlation between the La Jencia and Bloodgood Canyon tuffs at 28.78 to 28.36 my.

INTRODUCTION

Numerous studies have been made of the Mogollon–Datil volcanic field, but a comprehensive stratigraphic framework for the area has not been developed. Recent K–Ar dating and detailed mapping have greatly advanced understanding of the stratigraphy in various subregions of the volcanic field (e.g. Osburn & Chapin 1983a, b, Ratté et al. 1984, Elston 1984, Seager et al. 1982). However, accurate stratigraphic correlation between subregions has been hampered by imprecision of K–Ar and fission-track dating and by the discontinuous pattern of outcrops produced by Basin and Range faulting.

In this paper we propose a stratigraphic framework for the eastern Mogollon–Datil volcanic field that is based strictly on ignimbrites (ash-flow tuffs). The Mogollon–Datil ignimbrites are well suited to this purpose. They are regionally extensive, time-stratigraphic units that were erupted episodically throughout the Oligocene part of the Mogollon–Datil sequence. Ignimbrites can be most confidently correlated where physical continuity can be established by detailed mapping. Indeed, most of the stratigraphy developed in Mogollon–Datil subregions is based on detailed mapping of ignimbrite outcrops. Accurate correlation of ignimbrites becomes much more difficult, however, where continuous outcrops are not available, particularly between ranges separated by downfaulted basins.

Many long-distance correlations of Mogollon–Datil ignimbrites have been based upon lithology, a criterion which is undependable when used alone. Lithology of individual ignimbrite units may show lateral, vertical, and sectoral variations (Hildreth & Mahood 1985). Additionally, some distinct Mogollon–Datil ignimbrites are lithologically identical. Efforts to geochemically "fingerprint" individual ignimbrites have shown limited success (Bornhorst 1980).

This study uses paleomagnetism and high-precision $^{40}Ar/^{39}Ar$ dating of sanidine separates to assemble stratigraphic sequences of ignimbrites from well-mapped subregions into an integrated stratigraphic framework for the Mogollon–Datil volcanic field. Paleomagnetism has been proven to be a powerful tool for correlation of ignimbrites (Reynolds 1977, Hildreth & Mahood 1985). Lithologic correlations can be tested by comparing paleomagnetic directions. Ignimbrites, both welded and non-welded, commonly show uniform magnetizations which accurately record the geomagnetic-field direction during cooling soon after emplacement (Reynolds 1977, Grommé et al. 1972, Hoblitt et al. 1985, Best et al. 1973, Gose 1970). Secular variation of the geomagnetic field results in significant directional changes over periods of 100 years or less, and the probability of different ignimbrites recording identical field directions is low (Bogue & Coe 1981). In addition, magnetic polarity provides an opportunity to fit ignimbrite stratigraphy into the worldwide sequence of geomagnetic reversals. Paleomagnetic results reported here build on preliminary data reported by McIntosh (1983).

High-precision $^{40}Ar/^{39}Ar$ dating of pure sanidine separates provides a significant increase in relative error over conventional K–Ar and fission-track dating techniques. An initial study of five ignimbrite units from the Socorro area showed $^{40}Ar/^{39}Ar$ dating to be sufficiently precise to distinguish four units erupted within a 1.4 my period (Kedzie 1984, Kedzie et al. 1985). A relative error of about ± 0.15 my was indicated, although absolute error is limited to about ± 0.3 my by the accuracy of the conventionally determined K–Ar age of standards. The present study extends the $^{40}Ar/^{39}Ar$ dating technique to ignimbrites from throughout the eastern Mogollon–Datil volcanic field.

It must be emphasized that this paper represents only a progress report on a Ph.D. thesis underway at New Mexico Institute of Mining

& Technology. The quantity of dating and paleomagnetic work that has been completed varies widely among units. As this study progresses, some of the conclusions offered in this paper will undoubtedly change.

PALEOMAGNETISM

Field and laboratory work

Thirty-three ignimbrites from the Mogollon–Datil volcanic field were sampled for paleomagnetic analysis (Fig. 1, Tab. 1). Of these, at least 27 represent stratigraphically distinct units. Typically eight oriented core samples were field-drilled from each of 247 sites. Samples were oriented using sun and magnetic compasses. Standard-sized specimens (2.35 cm in diameter and 2.1 cm long) were subjected to alternating field (AF) demagnetization in a single-axis unit using peak fields of up to 40 milliteslas (mT). Selected samples were thermally demagnetized stepwise to a maximum of 725°C using a Schonstedt TSD-1. All remanence measurements were performed using a modified Schonstedt SSM-1 spinner magnetometer interfaced to a Northstar S-100 microcomputer. Paleomagnetic directions reported in this paper have been corrected for structural attitude. Because the study area extends over only 1.5° of latitude, paleomagnetic directions are compared directly instead of converting them to virtual geomagnetic poles.

Origin of remanence

Rock-magnetic studies and petrographic analyses indicate that most of the ignimbrite samples contain both magnetite and hematite. Thermomagnetic analyses of 11 samples have shown primary Curie temperatures characteristic of magnetite (540–590°C) and secondary Curie temperatures characteristic of hematite (610–700°C) (McIntosh 1983). Reflected-light studies of polished sections show that most samples contain phenocryst and groundmass magnetite which has been partially to entirely replaced by hematite to form martite. The martite in some

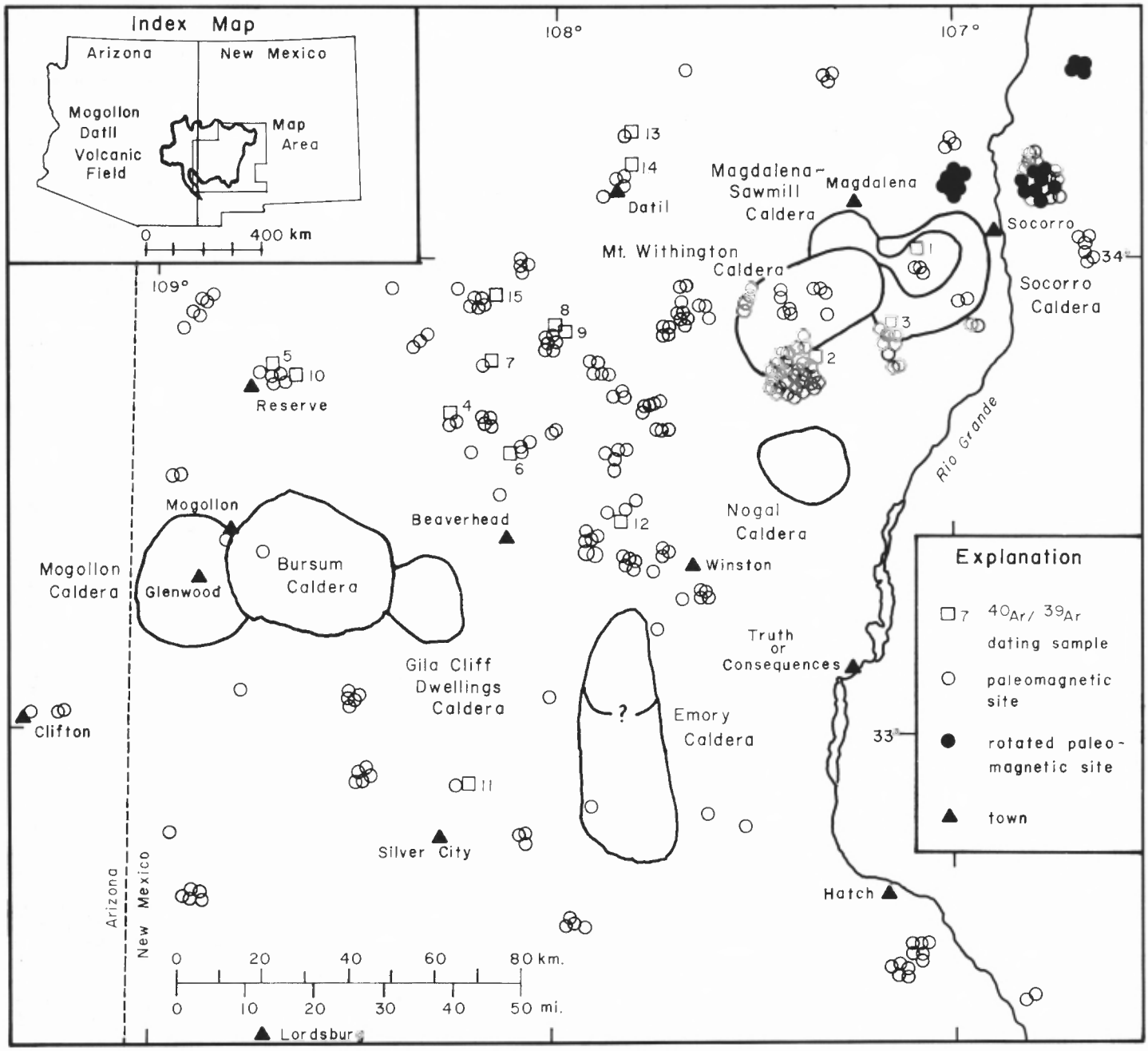


FIGURE 1—Location map for $^{40}Ar/^{39}Ar$ dating and paleomagnetic samples. Closed circles show sites in highly extended terrains where paleomagnetic data indicate tectonic rotations. Outlines of Mogollon, Bursum, and Gila Cliff Dwellings calderas after Ratté et al. (1984).

units contains lamellae of pseudobrookite. Also abundant are rutile-bearing titanohematite and microcrystalline hematite.

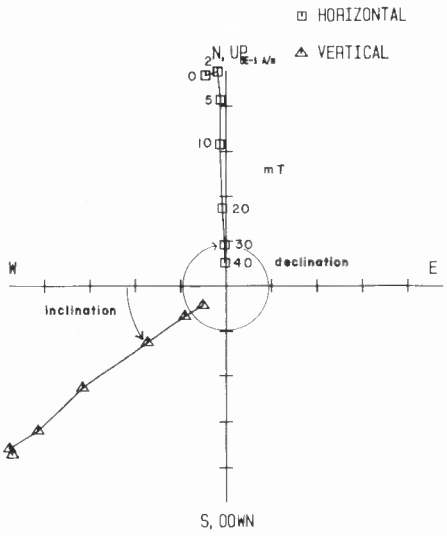
Pseudobrookite-bearing martite and rutile-bearing titanohematite are characteristic products of high-temperature (>700°C) deuteric oxidation (Haggerty 1976). Although martite and microcrystalline hematite are known to form over a wide range of temperatures (Walker et al. 1981), their association with pseudobrookite and rutile-bearing titanohematite suggests that they too are products of high-temperature deuteric oxidation which occurred during cooling of the ignimbrite.

Alternating field (AF) and thermal demagnetization of ignimbrite samples produced four general types of behavior, here designated types I, II, III, and IV. Samples from 49% of the 247 sites exhibited type I behavior. The natural remanent magnetization (NRM) vectors of these samples were well grouped within sites ($\alpha_{95} = 2–10°$). AF and thermal demagnetization reduced intensities but changed directions only slightly, typically resulting in modest improvements in within-site scatter ($\alpha_{95} = 1–5°$). Orthogonal demagnetization plots of type I behavior show nearly univectoral decay toward the origin (Fig. 2a–d). The rates at which intensity decreased, however, varied widely among samples. After demagnetization to 40 mT, remanence intensities ranged from 0.4 to 97% of NRM value (Fig. 2a, c). The fraction of remanence remaining after thermal demagnetization to 600°C showed a similar range of variation (Fig. 2b, d). Type I behavior is interpreted as a single-component thermoremanent magnetization acquired during cooling of the ignimbrites. The low-coercivity (<40 mT), low-temperature components are apparently carried by magnetite, whereas hematite carries the higher-

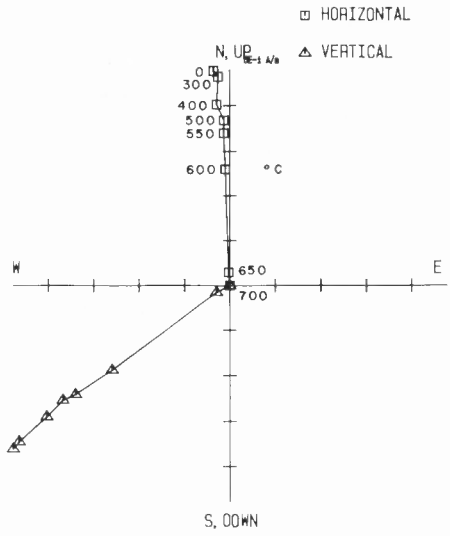
TABLE 1—Summary of $^{40}Ar/^{39}Ar$ and paleomagnetic data for ignimbrites of the eastern Mogollon–Datil volcanic field.

Unit	$^{40}Ar/^{39}Ar$ age(my)	nl	Paleomagnetism polarity	inc.	dec.	α_{95}	n2/n3	Volume (km3)	Caldera	Reference
Well Constrained Units										
SOUTH CANYON	27.36#	3	R	-28.9	200.2	4.4	23/37	700	Withington	7
LEMITAR	27.97*	1	N	39.6	357.1	6.2	12/21	450		7
Caronita Canyon	27.85	1	N	39.4	351.5	14.2	3/3	50	Sawmill/Magdalena	7
BLOODGOOD CANYON	28.36	1	R	-23.9	166.0	4.3	12/14	1000	Bursum	8
SHELLEY PEAK	28.52	1	R	-37.4	174.5	6.2	5/5	100-200	Gila Cliff Dw.?	8
VICKS PEAK	28.46#	2	R	-26.2	181.4	3.8	14/20	1050	Nogal	7
LA JENCIA	28.78#	4	R	-48.4	163.6	4.9	10/20	1250	Sawmill/Magdalena	7
DAVIS CANYON	29.03	1	R	-54.2	154.3	14.7	3/3	200-400	Gila Cliff Dw.?	8
HELLS MESA	32.04*	5	R	-60.7	158.4	6.7	6/12	1200	Socorro	7
BLUE CANYON	33.93	1	R	-36.9	143.4	10.4	3/4			7
ROCKHOUSE CANYON	33.93	1	R	-56.3	149.8	7.5	4/5			7
KNEELING NUN	35.28	1	R	-45.7	169.0	3.0	10/14	>900	Emory	2
Taylor Well			N	52.2	348.7	7.5	4/5			9
DATIL WELL	35.51	1	N	50.2	19.0	9.3	3/3			7
Partially Constrained Units										
Turkey Springs			R	-52.1	176.0	4.1	13/15			4
Triangle C Ranch	27.98	1	N	49.6	356.7	5.3	5/6			9
APACHE SPRING			R	-34.7	157.7	-	1/1	1200	Bursum	8
Garcia Camp			R	-29.9	181.2	-	1/2			10
Stiver Canyon			R	-52.7	172.6	-	1/2			12
CABALLO BLANCO			R	-48.0	178.2	12.9	4/5			3
BOX CANYON			R	-56.0	136.7	-	1/1			3
TADPOLE RIDGE	35.14	1	R	-72.2	174.1	-	2/2			5
FALL CANYON			R	-53.8	142.6	15.1	3/6			8
COONEY			R	-51.4	145.5	-	1/2	>100	Mogollon?	8
Bell Top 6			R	-51.0	131.4	-	2/2			1
Bell Top 5			R	-40.4	160.0	-	2/2			1
Bell Top 4			N	57.4	7.0	6.9	3/3			1
Bell Top 3			N	69.9	329.5	-	2/2			1
Bell Top 2			N	39.8	350.3	-	2/2			1
DONA ANA			N	44.4	329.7	-	2/2		Dona Ana	11
Rubio Peak 3			N	48.2	326.3	-	1/1			6
Rubio Peak 2			N	55.3	331.5	-	2/3			6
Rubio Peak 1			N	33.6	45.7	-	1/2			6

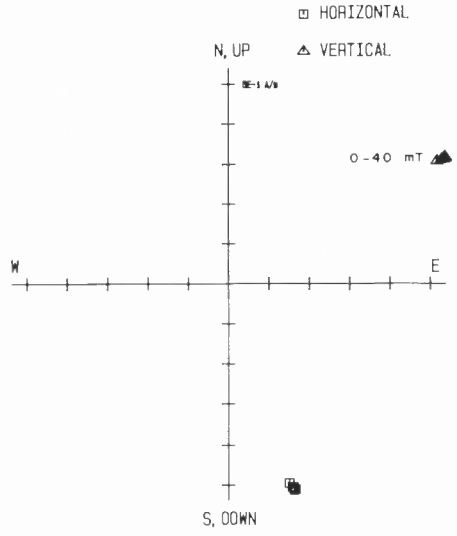
Explanation: units - capital letters denote formal unit names, lower case indicates informal names; age - mean of $^{40}Ar/^{39}Ar$ dates, * - from Kedzie et al, 1985, # - mean of dates from this study and from Kedzie et al, 1985; nl - number of samples used in the mean; dec. - mean declination; inc.- mean inclination; α_{95} - radius of cone of 95% confidence (not calculated for n2<3); n2 - number of sites used in the paleomagnetic mean; n3 - total number of sites paleomagnetically analyzed; volume - estimated volume of ignimbrite (not dense rock equivilent);
References: 1. Clemons, 1976; 2. Elston et al., 1975; 3. Elston, 1957; 4. C.A. Ferguson, unpubl. 1986; 5. Finnell, 1976; 6. R. Harrison, pers. com., 1986; 7. Osburn and Chapin, 1983a; 8. Ratte et al, 1984; 9. J. Ratte, Pers. com., 1986; 10. Richter, in press; 11. Seager et al, 1976; 12. Woodard, 1982.
Not included in this table are results from 20 sites in ignimbrite units of small extent or uncertain affinity.



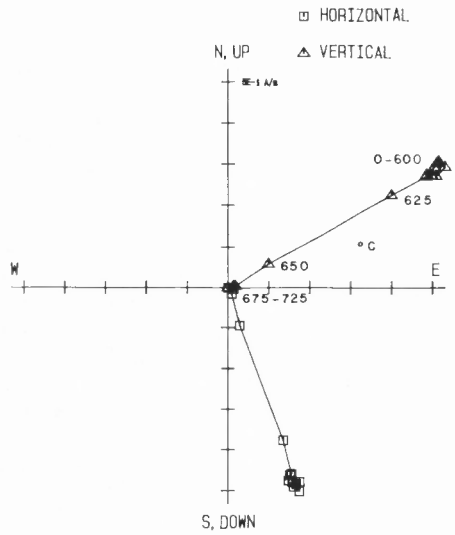
a, nm-22-4-03 Lemitar Tuff, AF



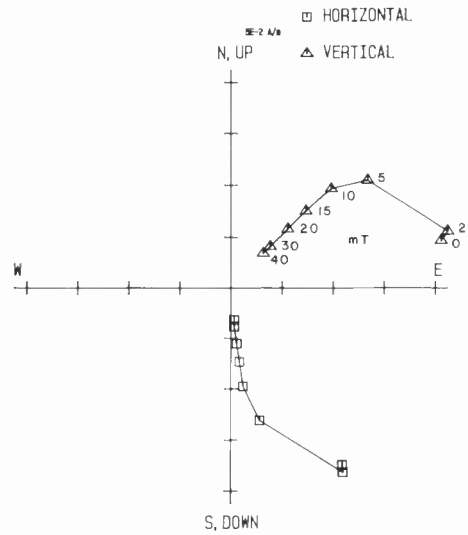
b, nm-22-4-02 Lemitar Tuff, thermal



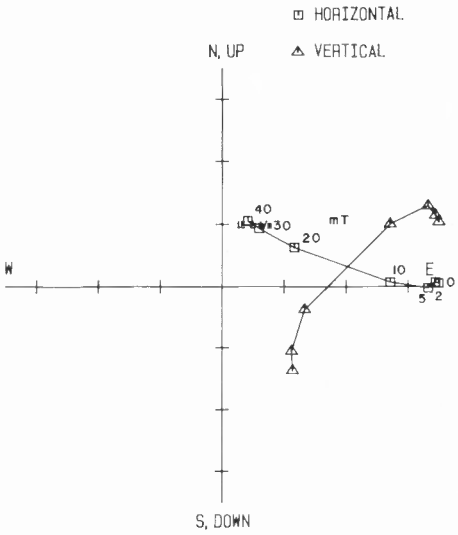
c, nm139-1-01 Bloodgood Canyon Tuff, AF



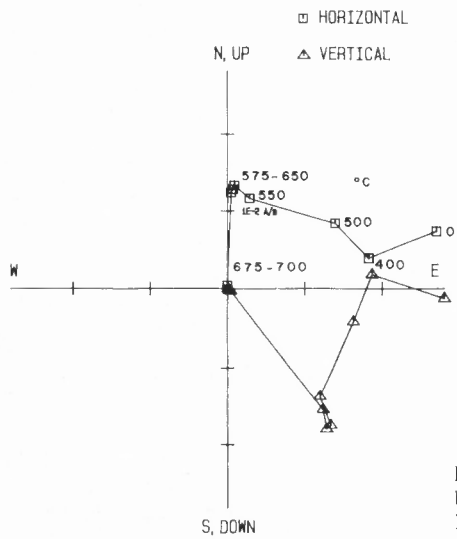
d, nm139-1-02 Bloodgood Canyon Tuff, thermal



e, nm-16-2-01 La Jencia Tuff, AF



f, nm145-1-01 Rockhouse Canyon Tuff



g, nm145-1-02 Rockhouse Canyon Tuff

FIGURE 2—Orthogonal plots showing demagnetization behavior of representative samples. **a, b:** Type I behavior —the low-coercivity, low-temperature components indicate a magnetite-dominated TRM. **c, d:**Type I behavior—the high-coercivity components indicate hematite-dominated remanence. **e:** Type II behavior—removal of lightning-induced IRM components. **f, g:** Type III behavior—multicomponent remanence composed in part of alteration CRM.

coercivity, higher-temperature components. The parallel nature of these two components, demonstrated by univectoral decay during demagnetization, supports the petrographic evidence that most or all of the hematite in these rocks formed deuterically.

Samples from 41% of the sites showed type II behavior. The NRM directions of these samples were relatively scattered ($\alpha_{95} = 10–180°$). AF demagnetization produced large directional changes accompanied by dramatic decreases in within-site scatter (most α_{95} values $<8°$). Orthogonal demagnetization plots of type II behavior show large directional changes between NRM and 10 or 20 mT, generally followed by univectoral decay toward the origin (Fig. 2e). The rates of intensity decrease associated with this univectoral decay showed a wide range of variation, similar to that of type I behavior. Type II behavior apparently indicates remanence composed of two components: (1) a TRM analogous to that associated with type I behavior, and (2) lightning-induced isothermal remanence (IRM) components. Most type II sites were collected from ridges or slopes exposed to lightning in areas where topographically protected outcrops were not available. In some type II sites, demagnetization at 40 mT did not completely remove IRM components, as reflected by α_{95} values in excess of 10°. AF demagnetization at higher fields will be required to completely isolate TRM components in samples from these sites.

Samples from 7% of the sites showed type III behavior. Their NRM vectors were reasonably well grouped, but AF and thermal demagnetization produced significant systematic changes in direction which generally increased scatter. Orthogonal plots of type III behavior demonstrate this multicomponent behavior (Fig. 2f, g). This type III behavior indicates that remanence components carried by magnetite and hematite are non-parallel. Possible explanations for multicomponent remanence of this nature include: (1) secular variation of the geomagnetic field during cooling of the unit, or (2) chemical remanence (CRM) components carried by hematite (or maghemite) formed after the unit cooled. Many of the sites showing type III behavior were collected from or near alteration zones.

Lastly, samples from 3% of the sites exhibited type IV behavior. All of these sites represent poorly welded, lithic-rich portions of ignimbrites. The NRM vectors of these sites were quite scattered ($\alpha_{95} = 29–180°$), but AF and thermal demagnetization improved scatter only slightly. Demagnetization behavior varied widely among the various samples of each site. Apparently, type IV behavior indicates that the ignimbrites were insufficiently hot to reset the remanence of included lithics. It is noteworthy that several other sites from unwelded, lithic-rich portions of ignimbrites showed well-grouped type I or type II behavior. Apparently, the temperature attained by the included lithics is not always reflected in the general field appearance of the ignimbrite.

In summary, samples showing type I or type II demagnetization behavior apparently carry strong identifiable components of TRM that accurately reflect the geomagnetic field at the time of cooling, shortly after emplacement. In samples showing type III and type IV behavior (about 10% of the sites), the original TRM is masked by other components.

Remanence directions and attitude problems

A mean paleomagnetic direction and cone of confidence were calculated for each site using the AF demagnetization level which produced minimum scatter, typically 30 or 40 mT. In general, site-mean directions were quite uniform within individual ignimbrite units (Fig. 3). There are, however, several exceptions to this uniformity. Some of these non-uniform site-mean directions are related to significant non-TRM components, shown by types III and IV demagnetization behavior, as discussed above. There are other cases, however, in which TRM-bearing samples (types I and II above) yield well-grouped site-mean remanence directions that are significantly different from the mean direction of other sites in the same unit. In some cases these anomalous sites reflect incorrect determination of structural attitude. Ideally, attitudes were determined from the top contact of ignimbrite units, a surface which probably was nearly horizontal at the time of emplacement (Ross & Smith 1961: 23). In practice, however, many attitudes were measured using pumice foliations, welding zonations, or lower contacts of units. The attitudes of these features are somewhat variable and may have deviated significantly from horizontal at the time of emplacement and welding. Much of the "noise" between the mean directions of various sites within individual ignimbrite units can be attributed to uncertainties in attitude.

In many cases, sites located in highly extended terrains show anomalous mean directions (Figs. 1, 4). These areas include the Lemitar Mountains, Joyita Hills, and Black Butte. These discrepancies are apparently related to net rotations about non-horizontal axes, possibly caused by listric faulting and associated multiple episodes of tilting (Chamberlin 1983). Regional ignimbrite sheets allow sensitive and reliable detection of local tectonic rotations. They are far better suited to this purpose than are sediments and local lava flows, in which the effects of tectonic rotation and secular variation cannot be separated.

An average paleomagnetic direction was calculated for each ignimbrite unit using site-mean data (Tab. 1, Fig. 5). Data from certain sites were rejected in calculating the unit averages. Rejected sites include type IV sites, type III sites with large CRM components, type II sites with unremoved IRM components, sites with poor attitude control, and sites from highly extended terrains (Figs. 1, 4). Cones of confidence have been calculated for units having three or more reliable site means (Tab. 1). In cases where five or more reliable site means were available, unit mean α_{95} values are less than 8°.

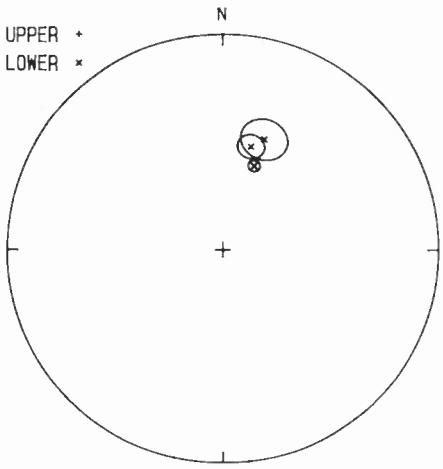
Paleomagnetic correlation

The simplest form of paleomagnetic correlation depends only upon the magnetic polarity of the units correlated. Because polarity is only a binary variable, the utility of simple polarity correlations is limited. The potential for more detailed correlations is given by the rapid secular variation of the geomagnetic field, provided the units correlated are sufficiently accurate paleomagnetic recorders.

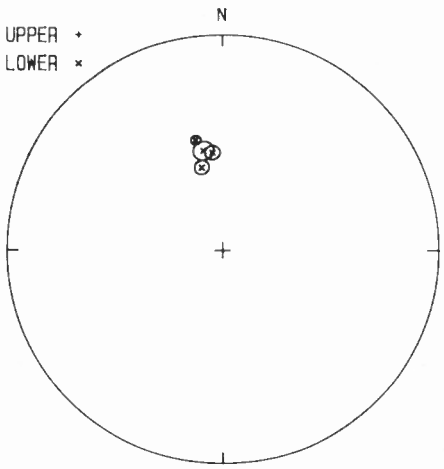
Most of the Oligocene Mogollon–Datil ignimbrites show reversed polarity (Tab. 1). Normal polarities are confined to the oldest units and to three young ignimbrites in the northern part of the volcanic field. Older normal units include the Datil Well Tuff, the three ignimbrites underlying the Kneeling Nun Tuff in the Winston area, the three lowest tuff members in the Bell Top Formation, and the Doña Ana Tuff. Younger normal units include the tuff of Caronita Canyon, the Lemitar Tuff, and the tuff of Triangle C Ranch, which overlies the Bloodgood Canyon Tuff near Pelona Mountain.

The potential for paleomagnetic identification and correlation varies widely among the ignimbrites of the Mogollon–Datil volcanic field. A number of the ignimbrites exhibit unique TRM directions which allow unambiguous paleomagnetic identification. These distinctive units include Datil Well, Vicks Peak, Bloodgood Canyon, and Tadpole Ridge Tuffs (Figs. 3, 5). The TRM directions of the remainder of the units fall closer to the average normal or reversed field directions for the Oligocene. It is still possible to paleomagnetically distinguish between many of these units (e.g. between the Kneeling Nun and Hells Mesa Tuffs), provided that structural attitudes can be accurately determined. However, some of the units (e.g. Kneeling Nun and Caballo Blanco Tuffs) are paleomagnetically indistinguishable.

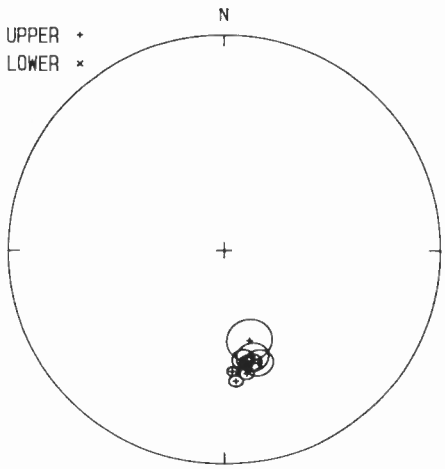
Paleomagnetic correlation has provided tests of existing correlations based on lithology and mapping criteria. In general, published stratigraphic columns for various subregions of the Mogollon–Datil volcanic field have held up well under these tests. Some new relationships, however, have been paleomagnetically demonstrated. Examples include: (1) The tuff of Turkey Springs (C.A. Ferguson unpubl.) has been found to overlie the lithologically identical South Canyon Tuff in the central San Mateo Mountains and the northern Black Range. This ignimbrite includes many of the exposures mapped as "upper member of the Railroad Canyon Tuff" by Fodor (1976). (2) The "lower member of the Railroad Canyon Tuff" of Fodor (1976) is actually the South Canyon Tuff in the Black Range and the Bloodgood Canyon Tuff in the Indian Peaks area. (3) The type Datil Well Tuff is paleomagnetically distinct from a lithologically identical unit identified as the Datil Well Tuff in the Jornada del Muerto area (G.R. Osburn unpubl.). The ignimbrite at Jornada del Muerto, here informally termed "tuff of Taylor Well," is actually younger than the Datil Well Tuff, as shown by sections



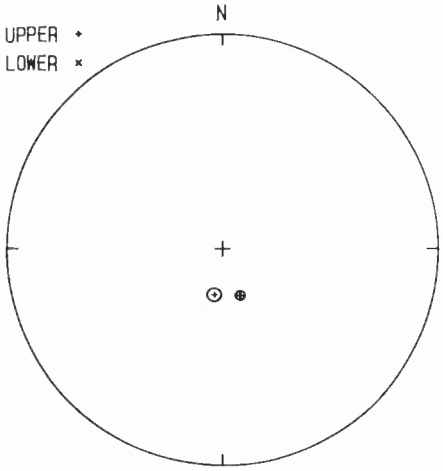
a, Datil Well Tuff



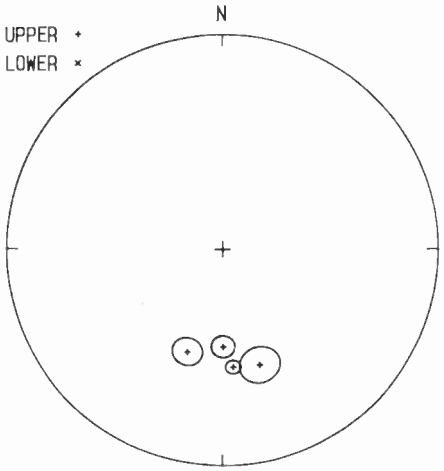
b, tuff of Taylor Well



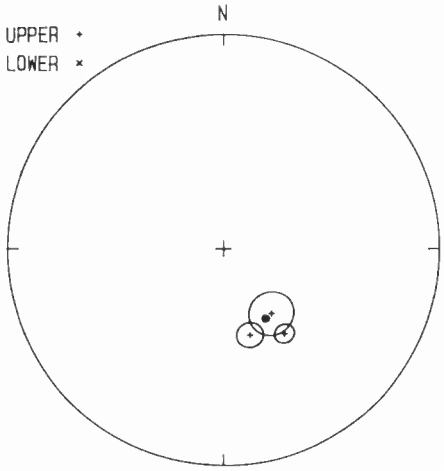
c, Kneeling Nun Tuff



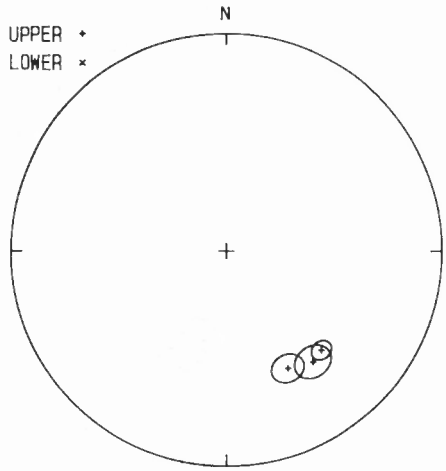
d, Tadpole Ridge Tuff



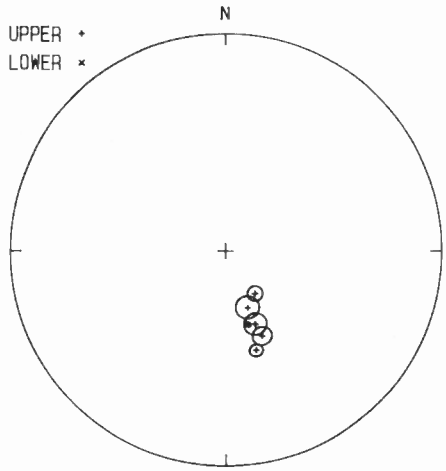
e, Caballo Blanco Tuff



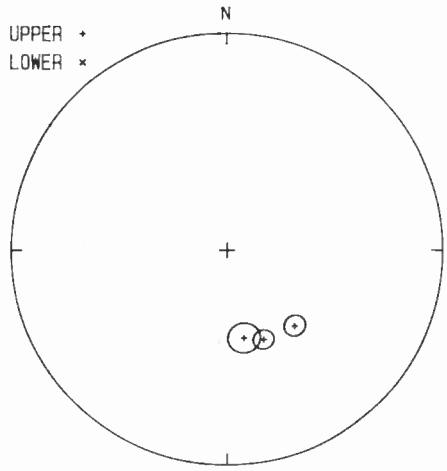
f, Rockhouse Canyon Tuff



g, Blue Canyon Tuff

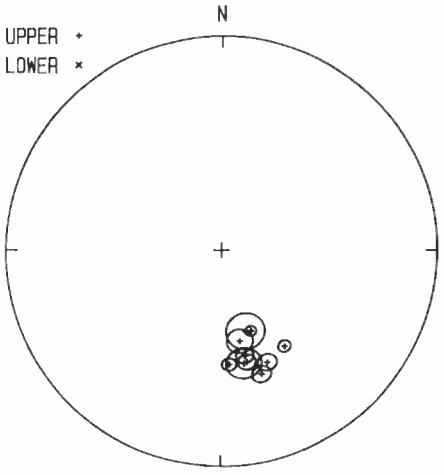


h, Hells Mesa Tuff

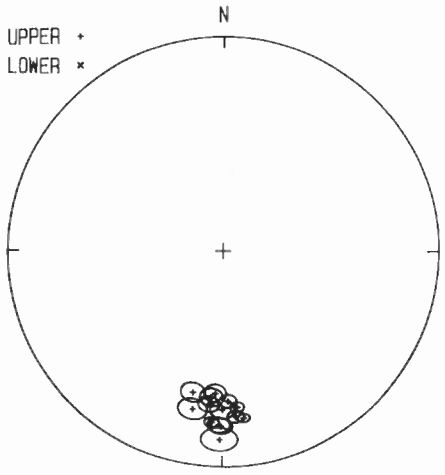


i, Davis Canyon Tuff

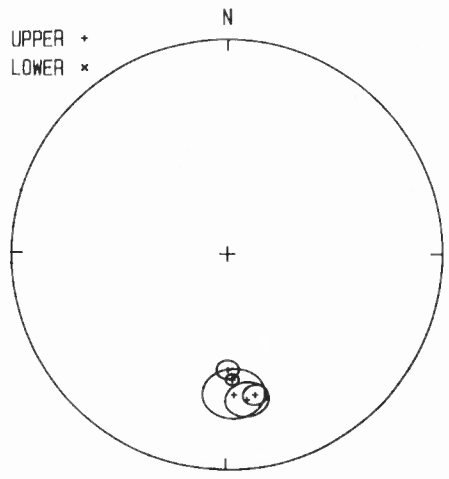
FIGURE 3—Site-mean paleomagnetic directions for Mogollon–Datil ignimbrite units. Crosses indicate mean directions and ellipses show cones of 95% confidence.



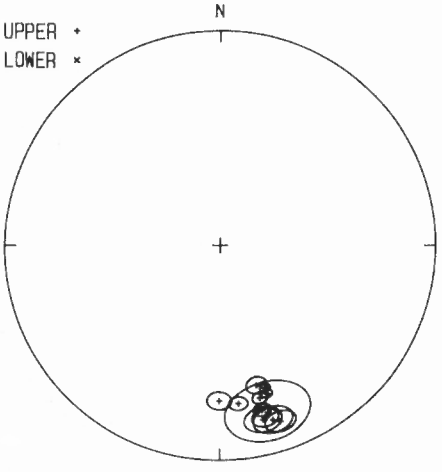
j, La Jencia Tuff



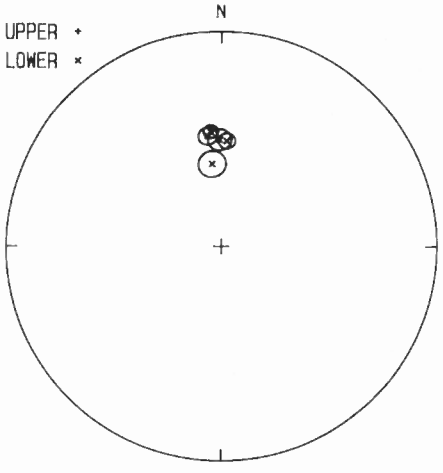
k, Vicks Peak Tuff



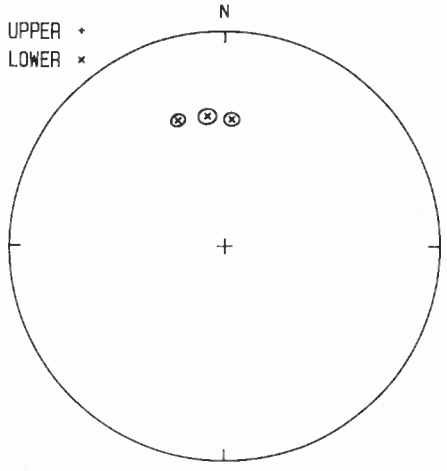
l, Shelly Peak Tuff



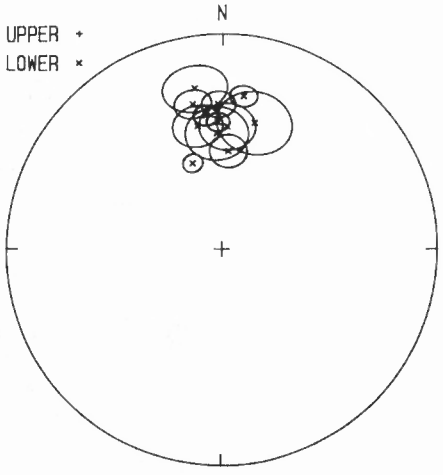
m, Bloodgood Canyon Tuff



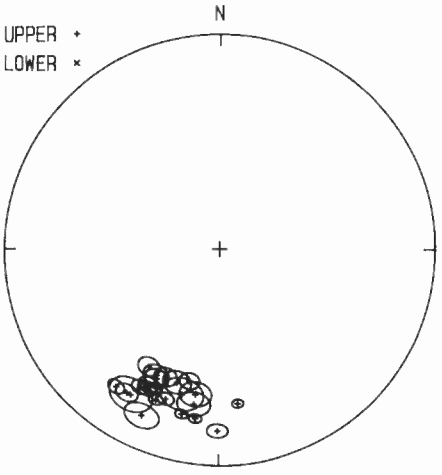
n, tuff of Triangle C Ranch



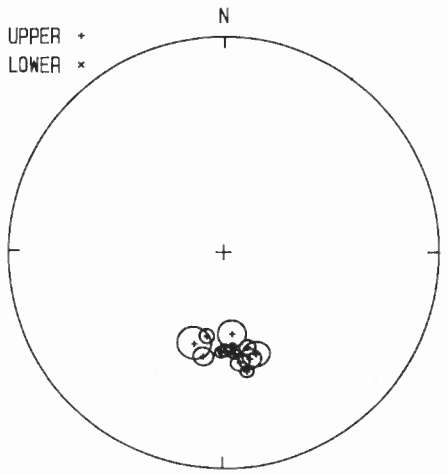
o, Caronita Canyon Tuff



p, Lemitar Tuff

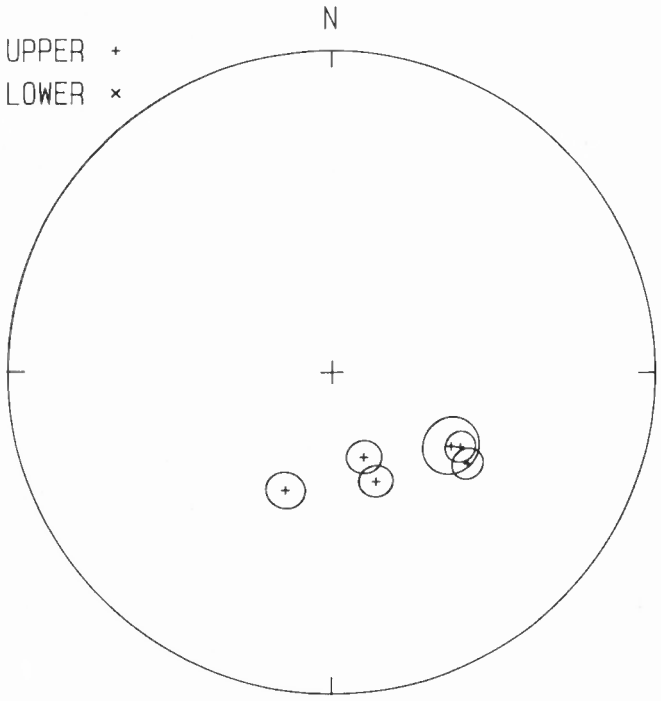


q, South Canyon Tuff

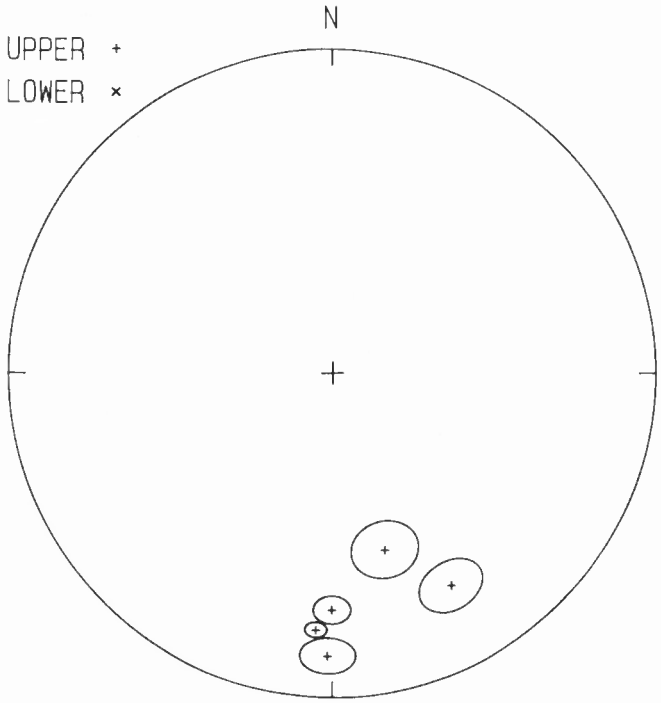


r, tuff of Turkey Springs

FIGURE 3 cont'd

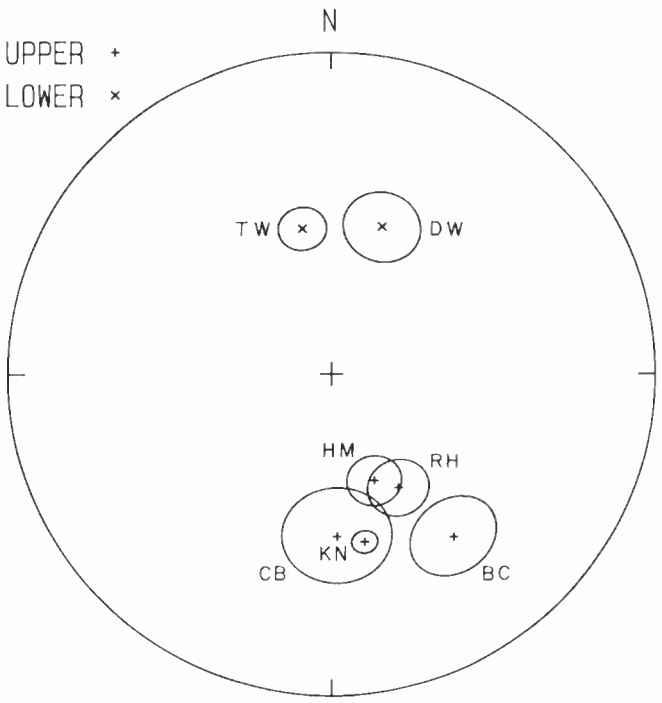


a, Hells Mesa Tuff, site means, highly extended terrain

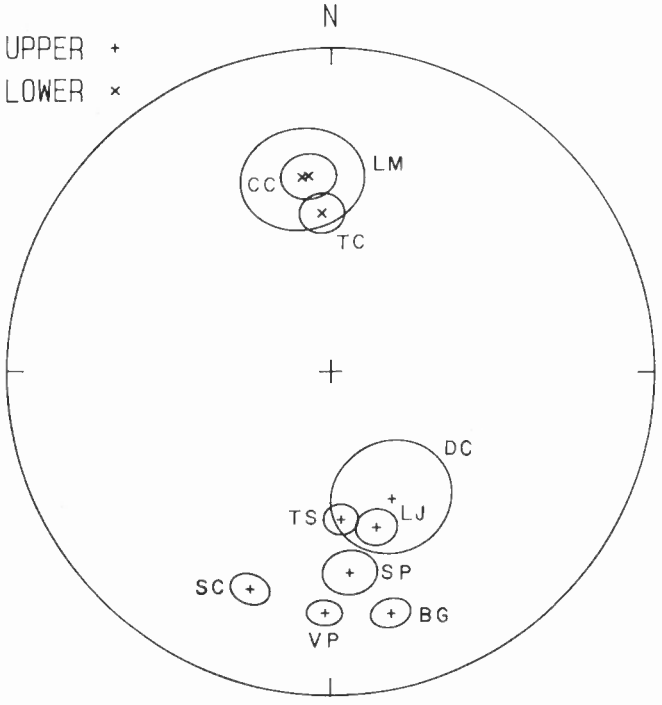


b, Vicks Peak Tuff, site means, highly extended terrain

FIGURE 4—Scattered mean paleomagnetic directions of sites located in highly extended terrain (Lemitar Mountains and Joyita Hills, see Fig. 1). Compare a and b with Figs. 3h and k, which show mean directions for sites in less extended areas. The paleomagnetic data from sites in highly extended areas indicate net rotations about non-horizontal axes, probably related to low-angle faulting and associated multiple episodes of tilting.



early and middle ignimbrites



late ignimbrites

FIGURE 5—Mean paleomagnetic directions and cones of 95% confidence for Mogollon–Datil ignimbrite units. Abbreviations: DW = Datil Well Tuff, TW = tuff of Taylor Well, KN = Kneeling Nun Tuff, CB = Caballo Blanco Tuff, RH = Rockhouse Canyon Tuff, BC = Blue Canyon Tuff, HM = Hells Mesa Tuff, DC = Davis Canyon Tuff, LJ = La Lencia Tuff, SP = Shelley Peak Tuff, BG = Bloodgood Canyon Tuff, CC = tuff of Caronita Canyon, LM = Lemitar Tuff, TC = tuff of Triangle C Ranch, SC = South Canyon Tuff, TS = tuff of Turkey Springs.

at Horse Springs and Horse Mountain, 30 km southwest of Datil, where both units are present.

Paleomagnetic correlation has also facilitated the tracing of some of the ignimbrites to their distal extremes, revealing previously unknown stratigraphic relationships with other units. Some of the more useful examples of such correlations are as follows: (1) The La Jencia Tuff has been identified in the Black Range, where it overlies the Stiver Canyon Tuff and underlies the Taylor Creek Rhyolite. (2) The Vicks Peak Tuff has been traced along the southern edge of the Plains of San Agustin and into the Tularosa River valley near Reserve. It overlies Davis Canyon Tuff and underlies Shelley Peak Tuff. (3) The Kneeling Nun Tuff extends to the Horse Springs area where it overlies Datil Well Tuff and underlies Rockhouse Canyon Tuff.

$^{40}Ar/^{39}Ar$ DATING

Technique

Conventional K–Ar and fission-track dating have been widely applied to Mogollon–Datil ignimbrite units, but both techniques have been limited by imprecision. K–Ar dating of biotite or sanidine separates has produced the most consistent results, but even these data show within-unit variations as large as several million years (e.g. Ratté et al. 1984: tab. 6).

An initial study of high-precision $^{40}Ar/^{39}Ar$ dating of mineral separates from five ignimbrites in the Socorro area (Kedzie 1984, Kedzie et al. 1985) demonstrated the technique to be far superior to conventional K–Ar and fission-track dating. The ages determined in the initial study show a relative error on the order of ± 0.15 my, and the potential resolution of the high-precision $^{40}Ar/^{39}Ar$ technique is even greater.

The general $^{40}Ar/^{39}Ar$ dating technique is well described elsewhere (Faure 1977, Dalrymple et al. 1981). The high precision attained in this study required several special procedures, similar to those used by Kedzie (1984) in the initial study: (1) Each of the 15 samples analyzed consisted of 0.1–0.27 g of 100% pure 60–120 mesh sanidine grains. All matrix glass was removed by ultrasonic probe. (2) Samples were irradiated for 20 hours in the constant-J portion of the central thimble of the USGS TRIGA reactor. Irradiation packages were monitored in detail by combinations of McClure Mountain hornblende standard MMhb-1 (Alexander et al. 1978) and Fish Canyon Tuff sanidine standard (Kunk et al. 1985). After the initial study, Hells Mesa Tuff sanidine was also employed as an internal standard. (3) Argon was extracted and analyzed at the USGS $^{40}Ar/^{39}Ar$ laboratory in Reston, Virginia. Age spectra were obtained from one to three splits from each sample using incremental RF induction heating in five to eight steps to temperatures of 1,500°C. Plateau ages (Fleck et al. 1977) were calculated for each split in which two or more contiguous gas fractions (a) comprised at least 50% of the total ^{39}Ar released and (b) showed ages statistically equivalent at the 95% confidence level, based on the critical value test of Dalrymple & Lanphere (1969).

The VG-Micromass 1200B spectrometer used in the analyses provided an analytical precision of $\pm 0.25\%$. The overall precision of the $^{40}Ar/^{39}Ar$ dating technique used in this study is estimated to be $\pm 0.50\%$ or better, providing a relative dating error for Oligocene samples of ± 0.12–0.19 my or better. The absolute error of dates, however, is limited by the accuracy of the conventional K–Ar dating of the monitor standards. This absolute error is about $\pm 1.0\%$, or about ± 0.24–0.37 my for Oligocene samples.

Results

Age spectra which satisfied plateau age criteria were obtained from one or more splits from 12 of the 15 samples analyzed (Tab. 2). A thirteenth sample narrowly missed meeting the plateau criteria. These plateaus represent 63–100% of the total released ^{39}Ar (Tab. 2), and most discordancies were limited to the initial and/or final heating steps (Fig. 6). Mean ages for each sample were calculated by averaging the plateau ages of splits. The $^{40}Ar/^{39}Ar$ dating results from this study are detailed in Tab. 2. Tab. 1 summarizes these results, together with the results of the initial study (Kedzie 1984, Kedzie et al. 1985).

The $^{40}Ar/^{39}Ar$ ages of ignimbrites dated in this study range from

TABLE 2—Results of $^{40}Ar/^{39}Ar$ dating of sanidine separates.

	Sample	Unit	np/nt	$\%^{39}Ar$	Age(my)
1.	78-6-1	South Canyon	1/1	89.8	27.37
2.	nm-81	South Canyon	0/1	42.6*	27.36
3.	nm-167	Caronita Canyon	1/2	67.9	27.85
4.	nm-158	Triangle C Ranch	2/2	75.4	27.98
5.	nm-95	Bloodgood Canyon	0/3	-	-
6.	nm-112	Bloodgood Canyon	1/3	72.5	28.36
7.	nm-149	Shelley Peak	2/2	80.1	28.52
8.	nm-143	Vicks Peak	1/3	63.1	28.47
9.	nm-146	La Jencia	2/3	91.1	28.86
10.	nm-96	Davis Canyon	2/2	100.0	29.03
11.	nm-102	Tadpole Ridge	1/1	89.0	35.14
12.	nm-110	Kneeling Nun	1/1	67.1	35.28
13.	81-12-6	Blue Canyon	2/2	81.1	33.93
14.	nm-85	Datil Well	2/2	86.4	35.51
15.	nm-90	Datil Well	0/2	-	-

Explanation: np/nt = number of splits yielding a plateau age / total number of splits; $\%^{39}Ar$ = percent of ^{39}Ar released in plateau, as defined in text; age = mean of planteau ages of splits; * = sample nm-81 barely failed to meet plateau criteria and is included as a preferred age; Sample locations, keyed to numbers at left, are shown in Fig. 1.

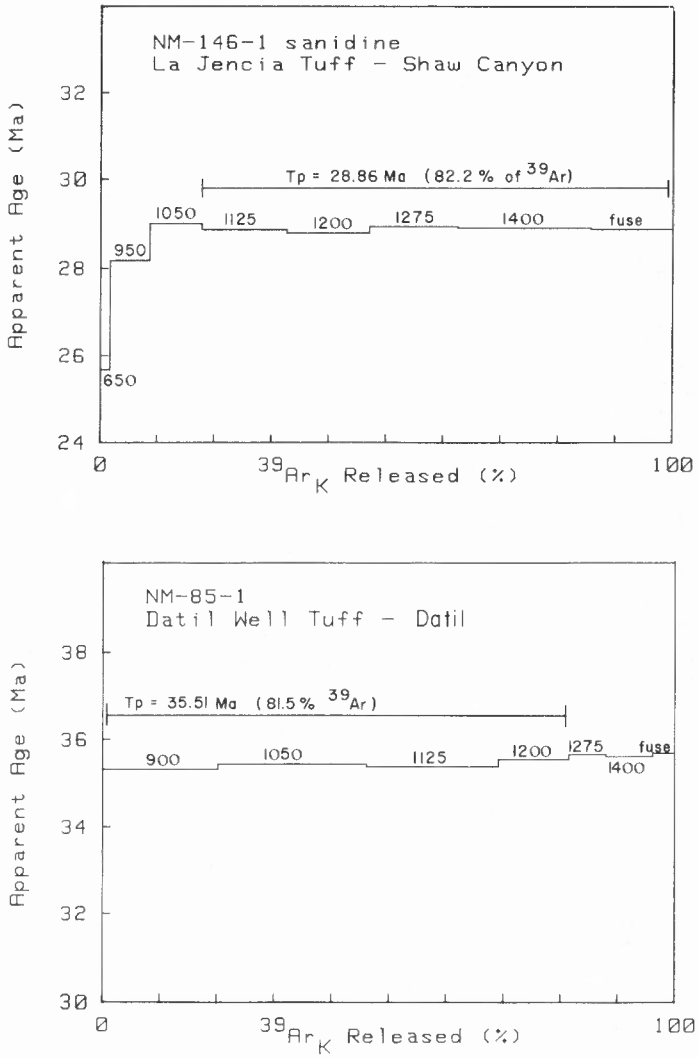


FIGURE 6—$^{40}Ar/^{39}Ar$ age spectra for two representative samples.

35.51 my to 27.36 my. Results from samples of the younger Socorro area ignimbrites show excellent agreement with results of the initial study (Kedzie et al. 1985). Ages from samples of the Vicks Peak and South Canyon Tuffs agree to within 0.01 my of the ages reported by Kedzie et al. (1985), although one of the South Canyon samples in this study (Tab. 2) failed, barely, to meet strict plateau age criteria. The age of the single La Jencia sample differs by only 0.1 my from the average La Jencia age reported by Kedzie et al. (1985).

In only two cases do the $^{40}Ar/^{39}Ar$ ages of this study violate stratigraphic relationships demonstrated by mapping and paleomagnetism. First, the 28.46 my age of the Vicks Peak Tuff is 0.06 my younger than the 28.52 my age of the overlying Shelley Peak Tuff. Second, the 27.85 my age of the tuff of Caronita Canyon is 0.12 my younger than the 27.97 my age of the overlying Lemitar Tuff. In both cases the discrepancies involve one or more ages determined from a single dated sample. Both discrepancies also fall within the 0.5% relative error estimated for the high-precision $^{40}Ar/^{39}Ar$ dating technique.

The $^{40}Ar/^{39}Ar$ ages summarized in Tab. 2 differ significantly from many individual conventional K–Ar and fission-track dates determined from Mogollon–Datil ignimbrite units. However, in cases where large numbers of conventional K–Ar dates have been obtained, their means show general agreement with the $^{40}Ar/^{39}Ar$ ages (e.g. Ratté et al. 1984: tab. 2).

The $^{40}Ar/^{39}Ar$ age data reported in this paper represent dates from only single samples of most of the ignimbrite units. Further dating of multiple samples from each unit will certainly improve the precision and reliability of the age determinations and provide improved estimates of the relative error of the high-precision $^{40}Ar/^{39}Ar$ dating technique. This relative error may also soon be improved by technical refinements now in progress at the USGS $^{40}Ar/^{39}Ar$ laboratory in Reston, Virginia.

STRATIGRAPHIC FRAMEWORK AND MAGNETOSTRATIGRAPHY

The ages of the 14 well-constrained Mogollon–Datil ignimbrites fall into three eruptive intervals separated by significant hiatuses. These eruptive intervals are here informally designated as early, middle, and late. Fig. 7 summarizes the ages and stratigraphic relations of these well-constrained units, as well as available data for partially constrained units.

The early eruptive interval extended from at least 35.51 my to at least 33.93 my. Well-dated ignimbrite units emplaced during this eruptive interval include the Datil Well Tuff (35.51 my) and Blue Canyon Tuff (33.93 my). The polarity of the Datil Well Tuff is normal, whereas the other three units are reversed.

The normal-to-reversed polarity transition that occurred at about 35.4 my between emplacement of the Datil Well and Kneeling Nun Tuffs provides a distinctive marker horizon that can be traced throughout many of the older Oligocene sections in the Mogollon–Datil volcanic field. In the Socorro area, the reversal is shown by ignimbrites within the Spears Formation. There the normally magnetized Datil Well Tuff and tuff of Taylor Well (informal name) are overlain by the reversed Rockhouse Canyon Tuff. In the Winston area, the reversed Kneeling Nun Tuff is underlain by a sequence of three normal ignimbrites in the Rubio Peak Formation. In the Goodsight–Cedar Hills depression, a reversal is present in the Bell Top Formation, where the three lower ignimbrite members (Bell Top tuffs 2, 3, and 4) are normal and the two upper ignimbrite members (Bell Top tuffs 5 and 6) are reversed. Although $^{40}Ar/^{39}Ar$ ages have not yet been obtained for any of the Bell Top tuffs, it is probable that the normal-to-reversed polarity correlates with the reversal between the Datil Well and Kneeling Nun Tuffs. In fact, paleomagnetic data suggest that Bell Top tuff 5 may represent a distal facies of the Kneeling Nun Tuff. The regional correlation of the 35.4 my normal-to-reversed polarity transition indicates that (1) the upper part of the Spears Formation is younger than Rubio Peak Formation in the Winston area, and (2) the lower part of the Bell Top Formation is equivalent to the Rubio Peak Formation in the Winston area.

The middle eruptive period is represented by only one well-dated unit, the Hells Mesa Tuff (32.04 my). This voluminous tuff (1,200 km^3) is the only ignimbrite known to have erupted in the period between 33.93 my and 29.03 my, although many other ignimbrite units have not yet been accurately dated. In the Socorro area, the eruption of the Hells Mesa Tuff was preceded by the eruption of the Blue Canyon Tuff (33.93 my) and followed by the eruption of the La Jencia Tuff (28.78 my). The data indicate two long hiatuses in ignimbrite activity preceding and following eruption of the Hells Mesa Tuff.

It is uncertain whether these hiatuses in ignimbrite activity extended throughout the Mogollon–Datil volcanic field. The eruption of the Davis Canyon Tuff (29.03 my) preceded the eruption of the La Jencia Tuff by about 0.25 my. At least three other major ignimbrite units (Box Canyon, Caballo Blanco, and Stiver Canyon Tuffs) were erupted in the southern part of the Mogollon–Datil volcanic field sometime between eruption of the Kneeling Nun Tuff (35.28 my) and the La Jencia Tuff (28.78 my). Portions of the unit or units mapped as the Fall Canyon Tuff (Ratté et al. 1984) may have also been erupted during this interval. Future $^{40}Ar/^{39}Ar$ dating of these units will reveal the extent of major ignimbrite hiatuses in the southern part of the volcanic field.

The late eruptive interval is represented by at least nine voluminous ignimbrites which were erupted in the brief interval between 29.03 and 27.36 my. These include ignimbrites erupted from calderas in both the Mogollon Mountains and Socorro area. Well-dated ignimbrites emplaced during this interval include Davis Canyon Tuff (29.03 my), La Jencia Tuff (28.78 my), Vicks Peak Tuff (28.46 my), Shelley Peak Tuff (28.52 my), Bloodgood Canyon Tuff (28.36 my), tuff of Caronita Canyon (27.85 my), Lemitar Tuff (27.97 my), tuff of Triangle C Ranch (27.98 my), and South Canyon Tuff (27.36 my). The combined volume of ignimbrites erupted during this brief 1.67 my interval totals at least 6,000 km^3 (Tab. 1, Fig. 8).

The 1.67 my interval of intense ignimbrite activity spanned three polarity intervals. The lower five well-dated units are reversed (Fig. 6, Tab. 1). These ignimbrites—Davis Canyon, La Jencia, Vicks Peak, Shelley Peak, and Bloodgood Canyon Tuffs—range in age from 29.03 to 28.36 my and together are exposed over much of the Mogollon–Datil volcanic field. Studied exposures of ignimbrites representing the overlying normal and reversed polarity zones are limited to the northern part of the volcanic field. The overlying normal-polarity interval is represented by three ignimbrites: the tuff of Caronita Canyon, the Lemitar Tuff, and the tuff of Triangle C Ranch, ranging in age from 27.85 to 27.98 my (Fig. 6, Tab. 1). Normal polarity has also been reported (Strangway et al. 1976) from the Jordan Canyon Tuff, which overlies the Bloodgood Canyon Tuff in the Gila Cliff Dwellings area. This unit also may have been erupted during the normal polarity interval near 28 my. The uppermost reversed-polarity interval is represented by the South Canyon Tuff (28.36 my) and the overlying tuff of Turkey Springs (not yet dated).

The stratigraphic framework described above demonstrates the highly episodic nature of ignimbrite eruptive activity in the Mogollon–Datil volcanic field. Fig. 8 summarizes the time distribution and volumes of well-dated Mogollon–Datil ignimbrites.

CORRELATION WITH THE SEA-FLOOR MAGNETIC-ANOMALY RECORD

For ease of discussion, the six polarity zones described above have been assigned the letters A through F, in ascending order (Figs. 7, 8). A and E represent the two normal-polarity zones, whereas the others are reversed. In spite of the high-precision afforded by $^{40}Ar/^{39}Ar$ dating, the duration and timing of most of these polarity zones are not yet well constrained. Polarity zones A, C, and F each contain only one well-dated unit, and the dates of the three units representing polarity zone E are all indistinguishable within the 0.15 my relative error of the $^{40}Ar/^{39}Ar$ dating method. At present, the best constrained features of the Mogollon–Datil magnetostratigraphy are (1) the age of the reversal between polarity zones A and B, bracketed between the eruption of the Datil Well Tuff (35.51 my) and emplacement of the Kneeling Nun Tuff (35.28 my), and (2) the duration of polarity zone D, which extended at least 0.67 my, from 29.03 my to 28.36 my (Fig. 8).

At the present stage of this study, the data are not sufficient to confidently correlate the Mogollon–Datil magnetostratigraphy with the sea-floor magnetic-anomaly record (Fig. 8). In the sea-floor record, the number and relative lengths of polarity intervals are well established, but the absolute ages of the intervals are not well constrained. At least 20 major polarity intervals are known from Oligocene sea-floor record, as compared to six from the Mogollon–Datil volcanic field. Mogollon–Datil reversed zone D may correlate with the 0.9 my long reversed interval preceding normal anomaly 10 in the sea-floor record (Fig. 8), but this correlation is little more than a guess.

With further work in the Mogollon–Datil volcanic field, the potential for reliable correlation with the sea-floor record is high. Particularly

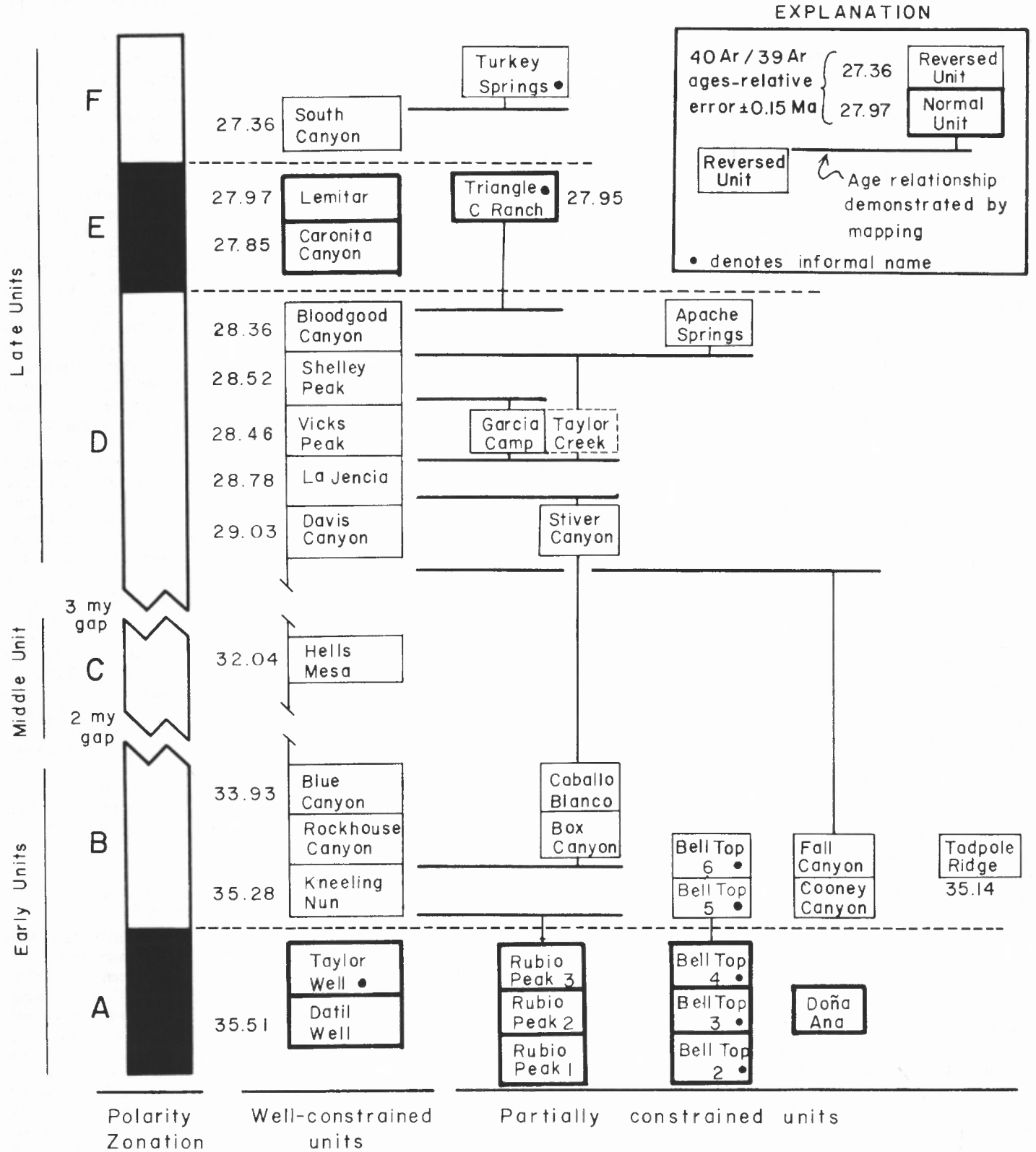


FIGURE 7—Stratigraphic framework for the Oligocene Mogollon–Datil volcanic field. Horizontal bars indicate stratigraphic relationships demonstrated by mapping and vertical lines show the age uncertainty allowed by these stratigraphic relationships.

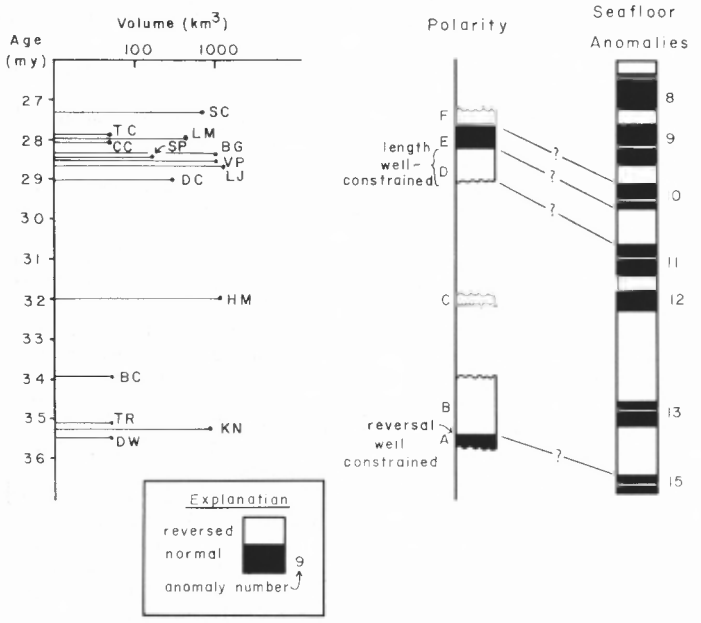


FIGURE 8—Distribution of volume and polarity of Mogollon–Datil ignimbrites through time. The volume–age relations demonstrate episodic nature of ignimbrite volcanism in this field. The suggested correlation of the ignimbrite-polarity record with the sea-floor record is tentative. The sea-floor anomaly scale is after Ness et al. (1980). Ignimbrite-unit abbreviations are same as in Fig. 5. Units for which volume estimates are not available are shown as 50 km^3.

characteristic are two distinctive long reversed intervals which occurred in the early Oligocene of the sea floor (reversed zones below normal anomalies 12 and 13 in Fig. 8). When the ignimbrite-based stratigraphic framework is more complete, the magnetostratigraphic record will be fleshed out by the addition of data from lava flows and local tuffs.

AGE OF THE TAYLOR CREEK RHYOLITES

Although this paper is focused on ignimbrite data, a discussion of the age of the Taylor Creek rhyolites is in keeping with the subject of this guidebook. Stratigraphic control of the Taylor Creek rhyolites is summarized in Fig. 7. In the southern part of the Taylor Creek area, rhyolite flows are underlain by the La Jencia Tuff (28.78 my) and overlain by the tuff of Garcia Camp and the Bloodgood Canyon Tuff (28.36 my) (Eggleston in press). In the northern part of the area, rhyolite flows are underlain by the tuff of Garcia Camp and overlain by the Bloodgood Canyon Tuff (Richter & Lawrence in press). The Shelley Peak Tuff (28.52 my) in this area overlies the Garcia Camp Tuff and may underlie dome-derived, block-and-ash flows (Richter & Lawrence in press). If these stratigraphic relations are correct, then the ages of Taylor Creek rhyolites are bracketed between 28.36 and 28.78 my, and the age of the tuff of Garcia Camp, and possibly some of the rhyolite flows, are bracketed between 28.52 and 28.78 my. The ages all fall within reversed-polarity interval D that extended from 29.03 to 28.36 my. This relationship agrees with the reversed polarity measured in the tuff of Garcia Camp (Tab. 1) and in two Taylor Creek Rhyolite flows.

CONCLUSIONS

1. Paleomagnetism and high-precision $^{40}Ar/^{39}Ar$ dating, coupled with existing detailed mapping, allow development of a reliable, ignimbrite-based stratigraphic framework for the Oligocene Mogollon–Datil volcanic field. Paleomagnetism aids in positive identification of ignimbrite units, particularly near their distal fringes, and $^{40}Ar/^{39}Ar$ dating yields ages with a relative error of ± 0.15 my or better. We have established the age and stratigraphic relations of 14 regional ignimbrites. Further work remains to be done on at least 13 more regional ignimbrites.

2. The stratigraphic framework developed so far suggests that Oligocene volcanicity in the Mogollon–Datil volcanic field was highly episodic. Ages of the well-dated units fall into three eruptive intervals separated by 2–3 my long ignimbrite hiatuses. These hiatuses are well established in the Socorro area, where $^{40}Ar/^{39}Ar$ ages have been obtained for most of the units. Further dating work will determine whether or not these ignimbrite hiatuses extend to the southern part of the field.

3. The earliest eruptive interval extended at least from 35.51 to 33.93 my. This interval includes the Kneeling Nun Tuff (35.28 my, >900 km^3) and ignimbrites within the Spears, Rubio Peak, and Bell Top Formations. A normal-to-reversed polarity transition which occurred about 35.4 my provides a marker horizon which can be traced throughout many of the older Mogollon–Datil stratigraphic sections. The position of this reversal indicates that (1) upper parts of the Spears Formation postdate the Rubio Peak Formation, and (2) the lower Bell Top Formation is equivalent in age to upper parts of the Rubio Peak Formation near Winston.

4. The middle eruptive interval, <33.93 to >29.03 my, encompasses only one well-dated ignimbrite: the Hells Mesa Tuff (32.04 my, 1,200 km^3), erupted from the Socorro cauldron. The Box Canyon, Caballo Blanco, Fall Canyon, and Stiver Canyon Tuffs in the southern part of the field may have also been erupted during this interval, but as yet none of these units has been precisely dated.

5. In the final eruptive interval, at least nine voluminous ignimbrites were erupted during the brief 1.67 my interval from 29.03 my to 27.36 my. These units, totaling at least 6,000 km^3, document a sequence of immense eruptions from calderas in the Mogollon Mountains and the Socorro area. This eruptive interval spanned three polarity intervals (reversed–normal–reversed).

6. Paleomagnetic data from sites in highly extended terrains commonly indicate net tectonic rotations about non-horizontal axes. Regional ignimbrites are much more sensitive and reliable recorders of such local rotations than are sediments or local lavas.

7. The ignimbrite paleomagnetic-polarity data cannot yet be confidently correlated with the sea-floor anomaly record, although it is possible that the Mogollon–Datil normal-polarity interval near 28.0 my may be equivalent to sea-floor normal-anomaly number 10. Further work will clarify this correlation.

ACKNOWLEDGMENTS

This work was supported by the New Mexico Bureau of Mines & Mineral Resources. Thanks to the many workers who shared their knowledge of portions of the Mogollon–Datil volcanic field, including Charles Ferguson, Rich Harrison, Ted Eggleston, Richard Chamberlin, Bill Seager, Rich Abitz, Wolf Elston, and Shiela Seaman. Thanks also to the many people who assisted in the field and lab, including Bob Andres and Scott Anderson. Critical reviews by Bill Seager, Phil Kyle, and Nelia Dunbar improved this paper.

REFERENCES

Alexander E.C., Mickelson G.M. & Lanphere M.A. 1978. MMHb-1: a new $^{40}Ar/^{39}Ar$ dating standard.—U.S. Geological Survey, Open-File Report 78-701: 6–8.

Best M.G., Shuey R.T., Caskey C.R. & Grant S.K. 1973. Stratigraphic relations of members of the Needles Range Formation at type localities in southwestern Utah.—Geological Society of America, Bulletin, 84: 3269–3278.

Bogue S.W. & Coe R.S. 1981. Paleomagnetic correlation of Columbia River basalt flows using secular variation.—Journal of Geophysical Research, 86: 11883–11897.

Bornhorst T.J. 1980. Major- and trace-element geochemistry and mineralogy of upper Eocene to Quaternary volcanic rocks of the Mogollon–Datil volcanic field, southwestern New Mexico (Ph.D. thesis).—University of New Mexico, Albuquerque, 1104 pp.

Chamberlin R.M. 1983. Cenozoic domino-style crustal extension in the Lemitar Mountains, New Mexico: a summary.—New Mexico Geological Society, Guidebook 34: 111–118.

Clemons R.E. 1976. Sierra de Las Uvas ash-flow field, south-central New Mexico. *In* Tectonics and mineral resources of southwestern North America.—New Mexico Geological Society, Special Publication 6: 115–121.

Dalrymple G.B. & Lanphere M.A. 1969. Potassium–Argon dating: principles, techniques, and application to geochronology.—W.H. Freeman & Co., San Francisco, 258 pp.

Dalrymple G.B., Alexander E.C. Jr., Lanphere M.A. et al. 1981. Irradiation of samples for $^{40}Ar/^{39}Ar$ dating using the Geological Survey TRIGA reactor.—U.S. Geological Survey, Professional Paper 1176: 55 pp.

Eggleston T.L. (in press). Geologic map of the Taylor Creek tin district, Black Range, New Mexico.—New Mexico Bureau of Mines & Mineral Resources, Open-file Report 177, scale 1:24,000.

Elston W.E. 1957. Geology and mineral resources of the Dwyer quadrangle, Grant, Luna, and Sierra Counties, New Mexico.—New Mexico Bureau of Mines & Mineral Resources, Bulletin 38: 88 pp.

Elston W.E. 1984. Mid-Tertiary ash flow tuff cauldrons, southwestern New Mexico.—Journal of Geophysical Research, 89: 8733–8750.

Elston W.E., Seager W.R. & Clemons R.E. 1975. Emory cauldron, Black Range, New Mexico: source of the Kneeling Nun Tuff.—New Mexico Geological Society, Guidebook 26: 283–292.

Faure G. 1977. Principles of isotope geology.—John Wiley & Sons, New York, 464 pp.

Finnell T.L. 1976. Geologic map of the Twin Sisters quadrangle Grant County, New Mexico.—U.S. Geological Survey, Miscellaneous Field Studies Map MF-779, scale 1:24,000.

Fleck R.J., Sutter J.F. & Elliot D.H. 1977. Interpretation of discordant $^{40}Ar/^{39}Ar$ age-spectra of Mesozoic tholeiites from Antarctica.—Geochimica et Cosmochimica Acta, 41: 15–32.

Fodor R.V. 1976. Volcanic geology of the northern Black Range, New Mexico. *In* Cenozoic volcanism.—New Mexico Geological Society, Special Publication 5: 68–70.

Gose W.A. 1970. Paleomagnetic studies of Miocene ignimbrites from Nevada.—Geophysical Journal of the Royal Astronomical Society, 20: 241–252.

Grommé C.S., McKee E.H. & Blake M.C. 1972. Paleomagnetic correlations and potassium–argon dating of middle Tertiary ash-flow sheets in eastern Great Basin, Nevada and Utah.—Geological Society of America, Bulletin, 83: 1619–1638.

Haggerty S.E. 1976. Oxidation of opaque minerals in basalts. *In* Oxide minerals.—Mineralogical Society of America, Short Course Notes, 3: H1–H100.

Hildreth W. & Mahood G. 1985. Correlation of ash-flow tuffs.—Geological Society of America, Bulletin, 96: 968–974.

Hoblitt R.P., Reynolds R.R. & Larson E.E. 1985. Suitability of non-welded pyroclastic-flow deposits for studies of magnetic secular variation: a test based on deposits emplaced on Mount St. Helens, Washington, in 1980.—Geology, 13: 242–245.

Kedzie L.L. 1984. High-precision $^{40}Ar/^{39}Ar$ dating of major ash-flow tuff sheets, Socorro, New Mexico (M.S. thesis).—New Mexico Institute of Mining & Technology, Socorro, 197 pp.

Kedzie L.L., Sutter J.F. & Chapin C.E. 1985. High-precision $^{40}Ar/^{39}Ar$ ages of widespread Oligocene ash-flow tuff sheets near Socorro, New Mexico.—EOS, Transactions of the American Geophysical Union, 17: 625.

Kunk M.J., Sutter J.F. & Naeser C.W. 1985. High-precision $^{40}Ar/^{39}Ar$ ages of sanidine, biotite, hornblende, and plagioclase from the Fish Canyon Tuff, San Juan volcanic field, south-central Colorado.—EOS, Transactions of the American Geophysical Union, 17: 636.

McIntosh W.C. 1983. Preliminary results from a paleo- and rock-magnetic study of Oligocene ash-flow tuffs in Socorro County, New Mexico.—New Mexico Geological Society, Guidebook 34: 205–210.

Ness G., Levi S. & Couch R. 1980. Marine magnetic anomaly timescales for the Cenozoic and Late Cretaceous: a precis, critique, and synthesis.—Reviews of Geophysics and Space Physics, 18: 753–770.

Osburn G.R. & Chapin C.E. 1983a. Nomenclature for Cenozoic rocks of the northeast Mogollon–Datil volcanic field, New Mexico.—New Mexico Bureau of Mines & Mineral Resources, Stratigraphic Chart 1.

Osburn G.R. & Chapin C.E. 1983b. Ash-flow tuffs and cauldrons in the northeast Mogollon–Datil volcanic field: a summary.—New Mexico Geological Society, Guidebook 34: 197–204.

Ratté J.C., Marvin R.F. & Naeser C.W. 1984. Calderas and ash-flow tuffs of the Mogollon Mountains.—Journal of Geophysical Research, 89: 8713–8732.

Reynolds R.R. 1977. Paleomagnetism of welded tuffs of the Yellowstone Group.—Journal of Geophysical Research, 82: 3677–3693.

Richter D.H. & Lawrence V.A. (in press). Geologic map of the Indian Peaks West quadrangle, Catron County, New Mexico.—U.S. Geological Survey, Miscellaneous Field Studies Map, scale 1:24,000.

Ross C.S. & Smith R.L. 1961. Ash-flow tuffs—their origin, geologic relations, and identification.—U.S. Geological Survey, Professional Paper 1294-E: E1–E12.

Seager W.R., Kottlowski F.E. & Hawley J.W. 1976. Geology of the Doña Ana Mountains, New Mexico.—New Mexico Bureau of Mines & Mineral Resources, Circular 147: 36 pp.

Seager W.R., Clemons R.E., Hawley J.W. & Kelley R.E. 1982. Geology of the northwest part of Las Cruces $1° \times 2°$ sheet, New Mexico.—New Mexico Bureau of Mines & Mineral Resources, Geological Map 53, scale 1:125,000.

Strangway D.E., Simpson J. & York D. 1976. Paleomagnetic studies of volcanic rocks from the Mogollon Plateau area of Arizona and New Mexico. *In* Cenozoic volcanism.—New Mexico Geological Society, Special Publication 5: 119–124.

Walker T.R., Larson E.E. & Hoblitt R.P. 1981. The nature and origin of hematite in the Moenkopi Formation (Triassic), Colorado Plateau: a contribution to the origin of magnetism in red beds.—Journal of Geophysical Research, 86: 317–333.

Woodard T.W. 1982. Geology of the Lookout Mountain area, northern Black Range, Sierra County, New Mexico (M.S. thesis).—University of New Mexico, Albuquerque, 95 pp.



The Snake mine and mill east of Hillsboro, ca 1905. R.W. Eveleth Collection.



Mamie Richmond mill along banks of Percha Creek east of Hillsboro, ca 1893. Photo courtesy of Black Range Museum.